SCA2003-26: APPLICATION OF NMR DIFFUSION EDITING AS CHLORITE INDICATOR

M. D. Hürlimann, A. Matteson, J. E. Massey, D. F. Allen and E. J. Fordham,
Schlumberger-Doll Research, Ridgefield, U.S.A.
F. Antonsen and H. G. Rueslåtten
Statoil Research Centre, Trondheim, Norway

This paper was prepared for presentation at the International Symposium of the Society of Core Analysts held in Pau, France, 21-24 September 2003

ABSTRACT

We present a nuclear magnetic resonance (NMR) based study on a series of sandstone cores from a major reservoir in the Norwegian Sea. The cores have varying amounts of chlorite and were prepared in different saturation states. NMR measurements were performed using the standard Carr-Purcell-Meiboom-Gill (CPMG) pulse sequence and the new diffusion editing method that is designed to separate diffusion and relaxation effects. This procedure generally results in more reliable S_w values and we demonstrate here that it can also be used to derive an indicator of chlorite content. Since the measurement of diffusion editing can be performed with logging tools, this technique can be used directly in a reservoir for the improved determination of saturation and to estimate the chlorite content, with important implications for the assessment of reservoir quality.

When the samples were saturated with a mixture of refined oil and brine it was generally difficult to separate the contributions of the two phases in the CPMG relaxation measurements. The relaxation time of the oil often overlapped significantly with the T_2 distribution of the brine signal. To overcome this problem, we used the technique of diffusing editing to obtain simultaneously diffusion and relaxation information and its correlation. This was achieved by preceding the standard short-echo-spacing CPMG sequence by an editing sequence that attenuates the amplitude of the signal according to diffusion in the applied gradient. In the current work, we implemented the diffusion editing by increasing the first two echo spacings systematically. Relaxation information is obtained from the signal decay after the diffusion encoding. This effectively orthogonalizes the diffusion and relaxation information and allows the extraction of diffusion – relaxation distribution functions. These two-dimensional $D - T_2$ maps can be used to extract information about important reservoir parameters such as water saturation, oil viscosity, wettability state and hydrocarbon-corrected bound-fluid volume.

For the samples with low chlorite concentration, the diffusion – relaxation distribution functions clearly separated the signal into oil and water contributions. For samples with higher chlorite concentrations, the $D - T_2$ maps showed an additional significant contribution at apparent diffusion coefficients in excess of bulk oil or water. In these

samples, the presence of chlorite gives rise to internal gradients in the adjacent pore space that exceeds the externally applied gradient. This leads to an increased diffusive decay that can be characterized by a large apparent diffusion coefficient. We found that the chlorite concentration in the sample is correlated with the fraction of signal that exhibits such large apparent diffusion coefficients.

INTRODUCTION

Studies on deeply buried reservoirs in the Norwegian Sea, Texas and Mississippi, have shown that porosity and permeability are reduced by the development of quartz overgrowths [1,2]. In some of these reservoirs' zones the development of quartz overgrowths is inhibited by grain-coating authogenic chlorite thus preserving high intergranular porosity. An optimum chlorite content is 4-5%, because this amount sufficiently covers the grain surfaces. Additional chlorite development occludes the pores and blocks the throats and is detrimental to permeability. Therefore, the assessment of the amount of chlorite in these reservoirs is critical for determining reservoir quality.

Nuclear magnetic resonance (NMR) has become an important method to evaluate petrophysical formation properties, such as porosity, permeability and water saturation, both in the laboratory and downhole [3]. The standard measurement of the distribution of T_2 relaxation times is based on the Carr-Purcell-Meiboom-Gill (CPMG) sequence. In a brine saturated formation, the T_2 distribution is usually directly related to the pore size distribution. It has been shown that the presence of paramagnetic minerals such as chlorite give rise to large internal magnetic field gradients. Diffusion in these gradients shifts T_2 relaxation distributions to shorter times [4,5]. This affects the value of the T_2 cutoff, used to determine the bound fluid volume, and consequentially the NMR derived permeability. NMR logging tools sample the near-wellbore region and it is important to separate the signal from the brine from that of the oil. However, the T_2 relaxation times of the different fluids often overlap which makes the determination of water saturation from relaxation measurements difficult. We have recently developed the new technique of *Diffusion Editing* [6] that is designed to separate diffusion and relaxation effects in order to extract diffusion – relaxation time distribution functions. We have demonstrated that this technique is suitable for borehole applications and can overcome the difficulty of brine/oil separation [7]. Here we demonstrate that for samples with low chlorite content, this new pulse sequence can easily differentiate oil from brine and determine the oil saturation quantitatively. In samples with large chlorite content, contributions with large apparent diffusion coefficients are observed. These contributions are caused by the large internal gradients and can be used to predict chlorite content. We show that this chlorite indicator correlates with the T_2 cutoff, the cementation exponent and the grain density. These quantities impact the log derived permeability, porosity and irreducible water saturation.

TECHNIQUE OF DIFFUSION EDITING

The basic concept of diffusion editing and one of its implementations are shown in Fig. 1. In the presence of a magnetic field gradient, data are acquired with at least two different

sequences, shown in the top panel. The first sequence is the standard CPMG sequence with minimal echo spacing, t_E. In the next sequence, the first two echo spacings are increased to $t_{E,1}$ and then followed by a long train of 180^o pulses with identical echo spacings t_E as in the first sequence. The initial time is used to *edit* the amplitude of the signal according to diffusion in the gradient. After this editing time, the pulse sequences are identical, resulting in identical relaxation times. However, the relative amplitude of each T_2 component depends on the extra diffusive decay during the initial interval as indicated in the second panel.

Compared to the first sequence, the signal of the second sequence has an amplitude that is reduced, or *diffusion-edited*, according to the diffusion coefficient of the fluid. The ratio of the amplitudes of the T_2 distribution depends only on diffusion because surface and bulk relaxation affects the signal in the two sequences the same way. The signal after the second echo is given by:

$$M(t,t_{E,1}) = \int\int dD\, dT_2\, f(D,T_2)\, \exp\{-t/T_2\}\, \exp\{-1/6\, g^2\, g^2\, D\, t_{E,1}^3\} \qquad (1)$$

Here $f(D,T_2)$ is the two-dimensional diffusion - T_2 probability density function, and g is the magnetic field gradient. Note that the kernel separates into two terms: $\exp\{-t/T_2\}$ only depends on the experimental time t and the relaxation time T_2; the second term, $\exp\{-1/6\, g^2\, g^2\, D\, t_{E,1}^3\}$, only depends on the different experimental time $t_{E,1}$ and the diffusion coefficient D. By measuring the signal for different initial echo spacings $t_{E,1}$, it is therefore possible to extract the diffusion coefficient and relaxation time separately. If measurements with two different values of $t_{E,1}$ are used (as shown in Fig. 1), it is possible to extract for every relaxation time T_2 an average diffusion coefficient. If more than two values of $t_{E,1}$ are used, it is possible to extract the distribution of diffusion coefficients for every T_2, resulting in the full D - T_2 map.

In our application, with extended samples in a static gradient, off-resonance effects modify Eq. (1) somewhat. These corrections are discussed in detail in Ref. [6]. Inversion of the data based on Eq.(1) to extract $f(D,T_2)$ implicitly assumes that the gradient g is known. Usually, it is simply given by the externally applied gradient, g_{ext}. However, when the formation contains significant amounts of magnetic minerals, the local gradient g_{loc} in the pore space can become noticeable. In such cases, the extracted apparent diffusion coefficient D_{app} for fluids exposed to large internal gradients exceeds the true diffusion coefficient: $D_{app} = (g_{loc} / g_{ext})^2\, D$. The presence of diffusion coefficients much in excess of the molecular diffusion coefficient can therefore be used to infer the presence of magnetic minerals, such as chlorite.

EXPERIMENTAL PROCEDURES

Samples and Petrophysical Measurements

Eight sandstone cores, with varying amounts of chlorite, were selected for this study. Core plugs were cleaned using the Soxhlet extraction technique. Material from the

annulus of these samples was homogenized and split. One portion was analyzed for mineralogy and the other for chemical content and grain density. Mineralogy was measured using Fourier Transform Infrared (FTIR) Spectroscopy [8]. The chemical analyses were performed by X-Ray Assay Laboratories (XRAL) in Don Mills, Ontario, Canada. Gas porosity and single-phase (gas) steady state permeability measurements were collected on the plugs. The eight plugs were then saturated in a pressure cell. Four terminal resistivity measurements were collected on the brine filled samples.

Oil and Brine Partial Saturation Procedure

Five samples were chosen for the partial saturation experiments. The oil, S3 (Canon Instruments viscosity standard), was chosen because its T_2 distribution most closely matched the filtrate of the oil based mud used in this well. Brine saturated core samples were first placed in cups filled with S3 oil and centrifuged for 24 hours at a differential pressure of about 65 psi, this is the *drainage* step. Next, the cores containing the irreducible water and S3 oil were each placed in a cup filled with 0.2 Ωm brine for seven days, this is the *spontaneous imbibition* step. After the spontaneous imbibition, the cores were each placed in a cup filled with brine of 0.2 Ωm resistivity and centrifuged at a differential pressure of 90 psi for 24 hours, this is the *forced imbibition* step. After forced imbibition, the five cores were placed in baths of D_2O. This was done so that the protons in the brine would exchange with the deuterium of D_2O and become NMR invisible, this is the *D_2O exchange* step. Wet and immersed weights were measured, and the oil and water saturations were calculated, after each saturation step.

NMR Experiments

NMR Relaxation Measurements

Nuclear magnetic resonance experiments were performed using a MARAN low field (2 MHz) hydrogen magnetic resonance instrument. The T_2 distributions were computed by evaluating the Carr-Purcell-Meiboom-Gill (CPMG) measurement. The inter-echo spacing used in these experiments was 240μsec and the delay time was 15 seconds. T_2 measurements were made after the eight samples were saturated with brine and after these samples were centrifuged for 24 hours at about 100 psi vs. air. The T_2 cutoff for each sample is the T_2 value of the brine saturated sample that corresponds to the porosity of the sample after it has been centrifuged. Five cores were then dried and re-saturated with brine and the T_2 measurements were collected after each step in the partial saturation procedure.

NMR Diffusion Editing Measurements

Diffusion editing measurements were performed in the fringe field of a 2T superconducting magnet. To simulate borehole applications, the samples were placed 0.5 m outside the magnet, resulting in a Larmor frequency of 1.76 MHz and a static gradient of 13.2 G/cm. At each saturation state of the sample, diffusion editing experiments were performed with 15 values of $t_{E,1}$ ranging between 0.4 ms and 48.4 ms. In all cases, 8000 echoes were acquired with an echo spacing t_E of 0.4 ms.

RESULTS AND DISCUSSION

The eight core samples are from a major reservoir in the Norwegian Sea. The samples are medium-grained and coarse-grained sands (Figs. 2 and 3). Petrographic and mineralogical analyses revealed that the composition of these sandstones is dominated by quartz with lesser amounts of feldspar, mica and clay (Table 1). The chlorite content for these samples ranges from 0 to 4.5 wt%. Chemical analysis shows that the iron content, expressed as equivalent Fe_2O_3, ranges from 0.28 to 4.56 wt%. The chlorite tends to be pore lining, although in some cases it also occludes the pores (Fig. 4). Chlorite rich samples tend to have higher grain densities, about 2.71 g/cm^3, than samples with low chlorite content whose grain densities are about 2.66 g/cm^3 (Table 1). Porosities range from 14 to 24 PU and the gas permeabilities range from 0.9 to 963 mD.

In Fig. 5, diffusion editing results are presented for a sample with moderate amounts of chlorite in different saturation states. In the middle column, the extracted diffusion – T_2 maps are displayed, while the left and right columns show the projections onto the T_2 and diffusion axis, respectively. The water and oil contributions clearly separate out in the diffusion – T_2 maps. The water signal lies on the dotted line at $D = 2.3\text{x}10^{-5}$ cm^2/s, the water diffusion coefficient, while the oil signal is centered at $D \sim 2.7\text{x}10^{-6}$ cm^2/s and $T_2 \sim$ 0.5 s, in good agreement with measurements on a sample of bulk oil. As expected, in the initial brine saturated state and after forced imbibition, the results show dominant water signals, with smaller water contributions after drainage and imbibition. The oil contributions also display the expected behavior. After forced imbibition, the results show a dominant water signal with a much weaker oil signal. After the D_2O exchange, most of the protons in the brine have been exchanged with deuterium and only the oil signal remains. The experimental result confirms the interpretation of the data from the previous step and demonstrates that the data inversion to produce D-T_2 maps is robust.

Note that not all the T_2 distributions shown on the left can be used to distinguish the oil from the water signal and to estimate the oil saturation, as the water and oil signals overlap significantly. However, in the diffusion dimension, there is a clear separation. Depending on the saturation state, the main peak in the diffusion distribution, *f(D)*, coincides either with the independently measured diffusion coefficient of water or oil, shown as blue and red lines, respectively. Using a cutoff of $8\text{x}10^{-6}$ cm^2/s, we can reliably determine the oil saturation, S_o. The gravimetrically determined oil saturations agree with the NMR based determinations based on the fractions of signal below this cutoff within 3 saturation units. These results confirm that diffusion editing can be used to determine oil saturation with overlapping T_2 distribution, even for samples with moderate amounts of chlorite. The diffusion editing method relies on sufficient diffusion contrast between oil and water. For waterwet formations with much lighter oils that have a reduced diffusion contrast with water, conventional T_2 distributions are expected to be adequate, since the T_2 distributions are less likely to be overlapping.

In the right columns of Fig. 5, the diffusion distributions *f(D)* systematically show extra contributions at high diffusion coefficients in addition to the two main peaks at diffusion

coefficients that coincide with those of bulk oil and water. As discussed above, these extra contributions are caused by internal gradients. This effect increases with increasing chlorite content. In Fig. 6, we present diffusion editing results for six different samples that are all brine saturated. The samples are ordered according to the measured iron content. In this figure, *f(D)* shows a distinct peak at the water diffusion coefficient plus additional contributions at more than a decade higher diffusion coefficients. As the iron (and chlorite) content increases, more and more of the weight in *f(D)* is shifted to higher apparent diffusion coefficients as a larger fraction of the fluid molecules are in close proximity to chlorite. This paramagnetic mineral produces local inhomogeneities in the magnetic field that are large compared with the externally applied gradient of 13.2 G/cm. It is interesting to point out that in the D-T_2 graphs of Fig. 6, the contributions showing water diffusion coefficient, i.e. signals representing fluid not in close contact to chlorite, have in general longer T_2 relaxation times than the contributions from fluid affected by internal gradients. The presence of chlorite increases the surface area of a pore and thus decreases its T_2. In addition, surface relaxation is supplemented by diffusion effects in the internal fields to further lower the measured relaxation times in pores coated or filled with chlorite [5].

The results in Fig. 6 suggest that we can quantify the internal gradient effect in diffusion editing using a diffusion cutoff of $5x10^{-5}$ cm^2/s. This cut-off is indicated as dotted line in the graphs of *f(D)* on the right hand column of Fig. 6. The numbers in the top right corner of these graphs indicate the fraction of the signal with apparent diffusion coefficients in excess of this cutoff, i.e. the fraction of the signal that is strongly affected by internal gradients. We use this fraction as our "diffusion editing indicator of chlorite".

In Fig. 7, this diffusion editing indicator is plotted versus chlorite concentration measured by FTIR spectroscopy and also versus iron concentration obtained by chemical analysis. Both graphs support the interpretation that the contribution at large apparent diffusion coefficients are related to chlorite concentration. In drainage or imbibition state (i.e. large oil saturations), the diffusion editing indicators are systematically lower than in the other two saturation states with high water saturation. This hydrocarbon effect is expected, as the diffusion coefficient of oil is lower, requiring a higher internal gradient to generate apparent diffusion coefficients in excess of the cutoff. A part of the scatter in the correlation with chlorite concentration is caused by the ±2% uncertainties in the FTIR determination of chlorite content. The correlation with chemical concentration of iron has less scatter, as the uncertainties for this determination are lower. However, it is important to keep in mind that the NMR based chlorite indicator is based on detecting magnetic field inhomogeneities on the pore level. They not only depend on the total iron content in the sample, but also on such properties as the types of iron bearing minerals (e.g. chlorite) and their specific surface area and spatial distribution. In the present case, the majority of the iron is contained in the chlorite.

The current experiments were performed at a magnetic field of 414 Gauss. Operating at a different field changes the amplitude of the internal gradients and therefore the sensitivity

to chlorite. At a lower field, accurate saturation determinations are possible for formations with chlorite concentrations higher than 2 wt%, whereas at higher fields, the characterization of chlorite concentrations below 2 wt% is improved.

The usefulness of the new chlorite indicator can be assessed by how well it correlates with important petrophysical quantities that are affected by chlorite and not easily measured directly in the borehole. In Fig. 8, we show the correlation between the chlorite indicator and three different quantities: the T_2 cutoff to determine the bound fluid, the cementation exponent, m, and the grain density. The first graph shows a correlation that is consistent with expectations: as the chlorite content increases, relaxation times decrease and the T_2 cutoffs decrease. In the second graph the results, for each saturation state, also indicate that with increasing chlorite content, the cementation exponent m increases due to increased tortuosity in the pore space. Both these quantities are important input parameters for log based permeability estimates. The grain density is directly affected by the heavy chlorite mineral and accurate values of ρ are needed for reliable porosity determination from density measurements.

CONCLUSIONS

We demonstrate that diffusion editing is a powerful new technique to evaluate cores with varying amounts of chlorite. This technique can be used both downhole or in the laboratory and measures the correlation between diffusion and relaxation effects. For samples with low to moderate chlorite content [up to 3 wt%], it has been used to determine accurately the water saturation at different saturation states, despite the fact that the oil T_2 had a significant overlap with water. This is achieved by taking advantage of the contrast in diffusion coefficients between the two fluids.

Higher chlorite content in the samples produces significant magnetic field inhomogeneities in the pore space, which is manifested by apparent diffusion coefficients that greatly exceed the true diffusion coefficients of the fluids. This effect prevents the application of this technique for saturation determination in these samples, but it can be used as a quantitative chlorite indicator. Accurate determination of chlorite in the formation is crucial to assess reservoir quality. In formations where chlorite has coated the grain surfaces, the development of quartz overgrowths is inhibited and porosity is preserved. We demonstrate that the new chlorite indicator can be used to estimate the T_2 cutoff for bound fluid, the cementation exponent and the grain density. These parameters are essential to extract accurately log-based petrophysical parameters, including porosity, permeability, water saturation and NMR based estimates of initial water cut.

ACKNOWLEDGEMENTS

The authors are grateful to Statoil for permission to publish these results and to Statoil and Schlumberger management for their support of this project. We also thank Wave Smith, Phil Frulla, Marina Polyakov and Mike Herron of Schlumberger-Doll Research for their petrophysical and mineralogy measurements.

REFERENCES

[1] Ehrenberg, S.N., "Preservation of Anomalously High Porosity in Deeply Buried Sandstones by Grain-Coating Chlorite: Examples from the Norwegian Continental Shelf," *AAPG Bulletin*, (July 1993) v. 77, No 7, p. 1260-1286.

[2] Thompson, A., Stancliffe, R.J., Shew, R.D., "Reservoir Quality, Sedimentary Source, and Regional Aspects of Norphlet Formation, South State Line Field, Greene County, Mississippi," *AAPG Bulletin*, (1987) v. 71, p.622.

[3] Kenyon, W.E., "Petrophysical Principles of Applications of NMR Logging," *The Log Analyst* (1997) 38, No. 2, 21.

[4] Rueslåtten, H., Eidesmo, T., Slot-Peterson, C., White, J., "NMR Studies of an Iron-Rich Sandstone Oil Reservoir." Proceedings of *International Symposium of the Society of Core Analysts*, the Hague (1998), paper SCA 9821.

[5] Zhang, G. Q., Hirasaki, G., House, W. V., "Diffusion in Internal Field Gradients," Proceedings of *International Symposium of the Society of Core Analysts*, the Hague (1998), paper SCA 9823.

[6] M. D. Hürlimann, L. Venkataramanan, and C. Flaum, "The diffusion - spin relaxation time distribution as an experimental probe to characterize fluid mixtures in porous media", *J. Chem. Phys.*, (2002) v.**117**, p. 10223-10232.

[7] M. D. Hürlimann, L. Venkataramanan, C. Flaum, P. Speier, C. Karmonik, R. Freedman, and N. Heaton, "Diffusion-Editing: New NMR Measurement of Saturation and Pore Geometry", Procedings of *SPWLA 43rd Annual Logging Symposium*, Oiso, Japan (2002), paper FFF.

[8] Herron, M. M., Matteson, A., Gustavson, G., "Dual-Range FT-IR Mineralogy and the Analysis of Sedimentary Formations," Proceedings of *International Symposium of the Society of Core Analysts*, Calgary (1997), paper SCA 9729.

Table 1. Petrophysical and mineralogy data for the eight samples.

Sample	Porosity	Perm	r	m	T_2 cutoff	Fe_2O_3	Quartz	Feldspars	Chlorite	Illite Smectite	Muscovite	Other
	%	mD	g/cm3		ms	wt%	wt%	wt%	wt%	wt%	wt%	wt%
1	13.8	52.3	2.66	2.0	22.2	0.62	90.3	3.2	0.0	3.1	2.3	1.0
2	11.0	371.0	2.65	1.8	67.8	0.28	88.2	7.7	0.6	1.8	0.0	1.7
3	19.5	302.0	2.66	1.8	43.2	0.68	83.9	2.8	2.1	1.8	3.4	6.1
4	17.5	963.0	2.66	1.7	48.0	0.60	87.2	1.4	2.7	0.9	2.5	5.4
5	14.0	0.9	2.72	2.1	23.0	4.14	78.9	2.8	3.9	2.9	5.3	6.3
6	22.9	60.1	2.68	2.2	20.8	2.47	82.7	3.1	4.1	3.0	4.3	2.8
7	22.4	55.6	2.72	2.2	15.8	4.56	76.2	2.6	4.2	3.8	4.1	9.1
8	23.9	387.0	2.71	2.1	12.5	4.23	81.0	3.4	4.5	4.1	2.8	4.3

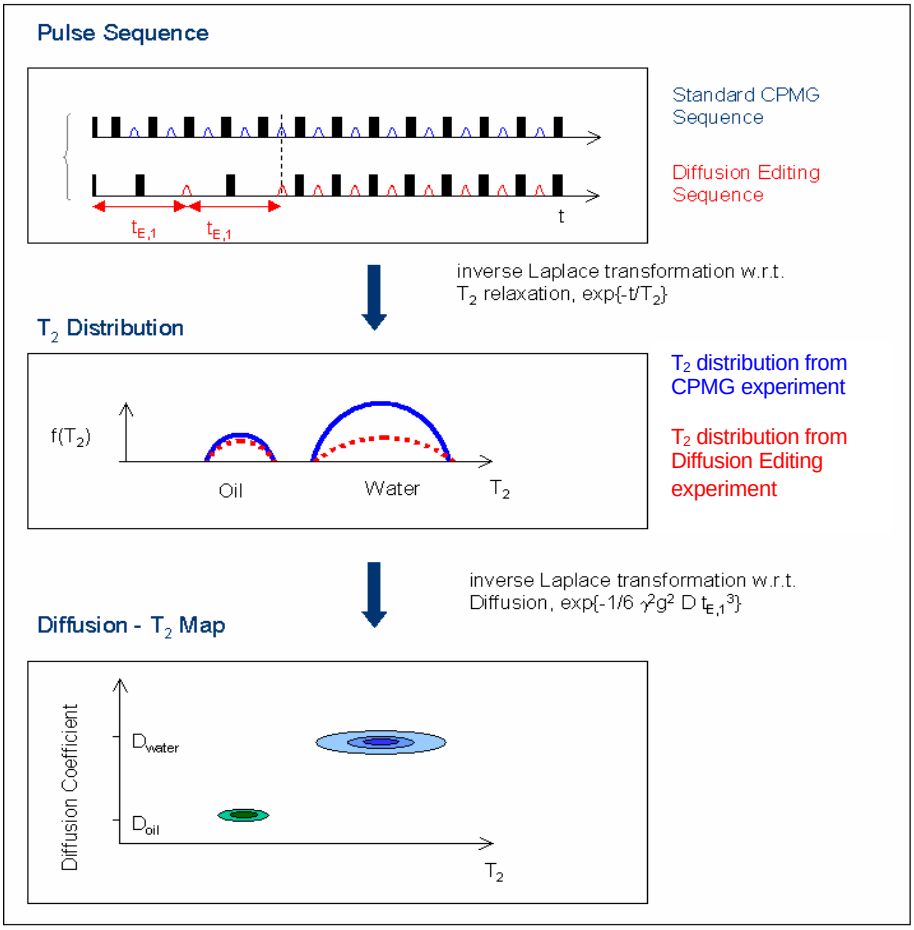

Figure 1. Principle of diffusion editing. The top panel shows the pulse sequences, the middle panel shows the extracted T_2 distributions from the different acquisitions, and the bottom panel shows the resulting Diffusion – T_2 maps. Details on the data inversion and implementation in inhomogeneous fields are given in Ref. [6].

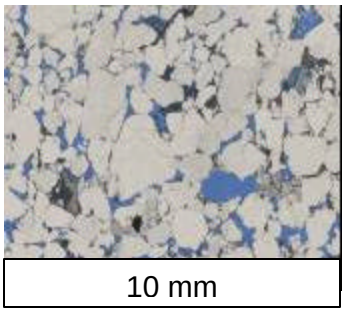

Figure 2. Thin section image of a coarse-grained sand (sample #4).

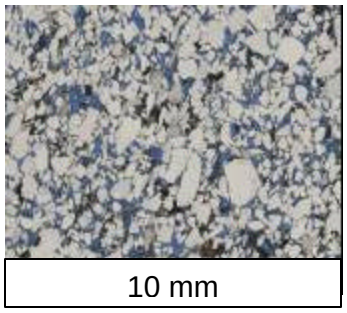

Figure 3. Thin section image of a medium-grained sand (sample #8).

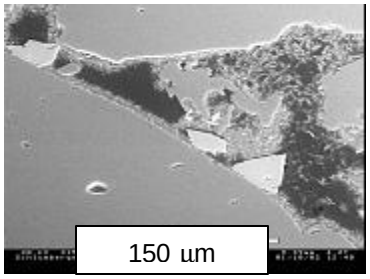

Figure 4. SEM image of pore lining, and pore occluding, chlorite in sample #8.

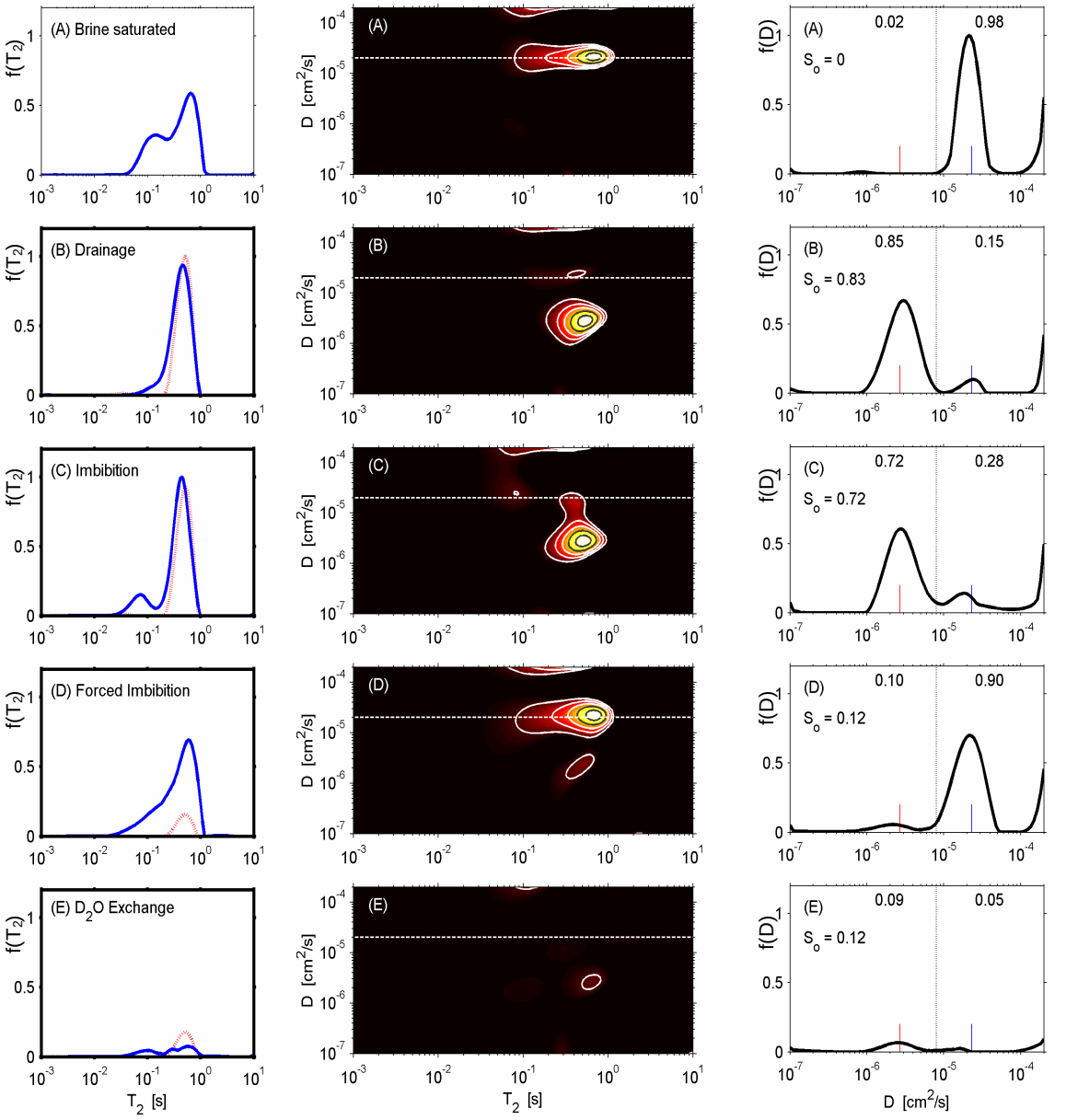

Fig. 5. Diffusion editing results for sample #4 under different saturation states. In the middle, D - T_2 maps are shown. On the left and right, the corresponding T_2 and D distributions are shown, obtained by projecting the maps onto the two different axes. In the D - T_2 maps, the dashed line indicates the diffusion coefficient of water and the contour lines are at 10, 30, 50, 70, and 90% of maximum, respectively. In the $f(T_2)$ graphs, the dashed line shows the T_2 distribution of bulk oil, scaled according to oil saturation. In the $f(D)$ graphs, the short lines show D of oil and water, whereas the dashed line shows the cutoff used to separate oil and water signal. The NMR derived values of S_o and S_w are shown on top, the gravimetrically determined value of S_o is given on the left.

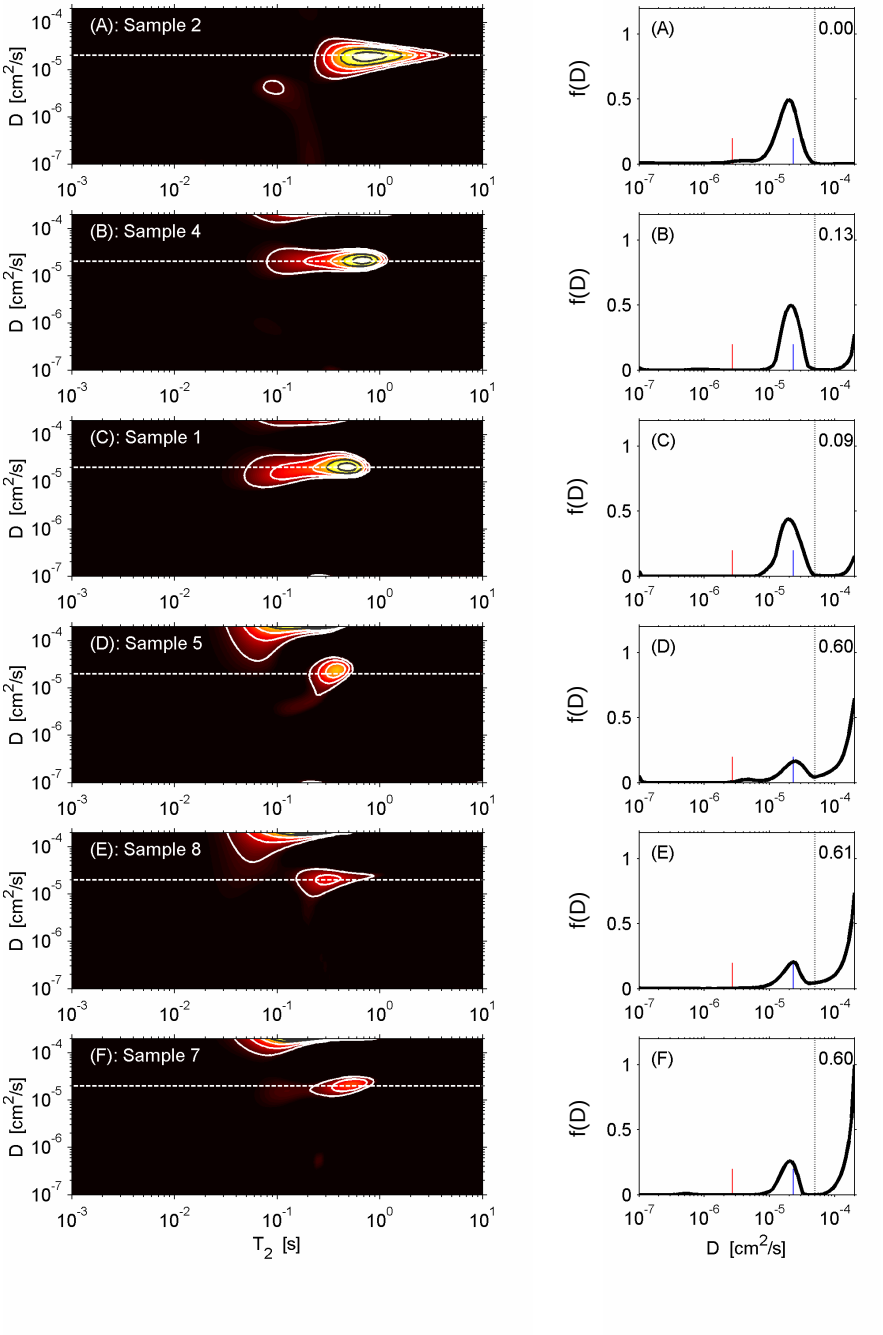

Figure 6. Diffusion editing results for six different samples that are all brine saturated. On the left, diffusion – T_2 maps are shown with the dashed lines indicating the molecular diffusion coefficient of water. On the right, the diffusion distributions *f(D)* are shown, obtained by projecting the D-T_2 maps onto the diffusion axis. The dashed lines show the cutoff used for chlorite indicator. The short red and blue lines indicate the diffusion coefficients of oil and water, respectively. The number on right is the fraction of the signal above the *D* cutoff, i.e. the "diffusion editing chlorite indicator".

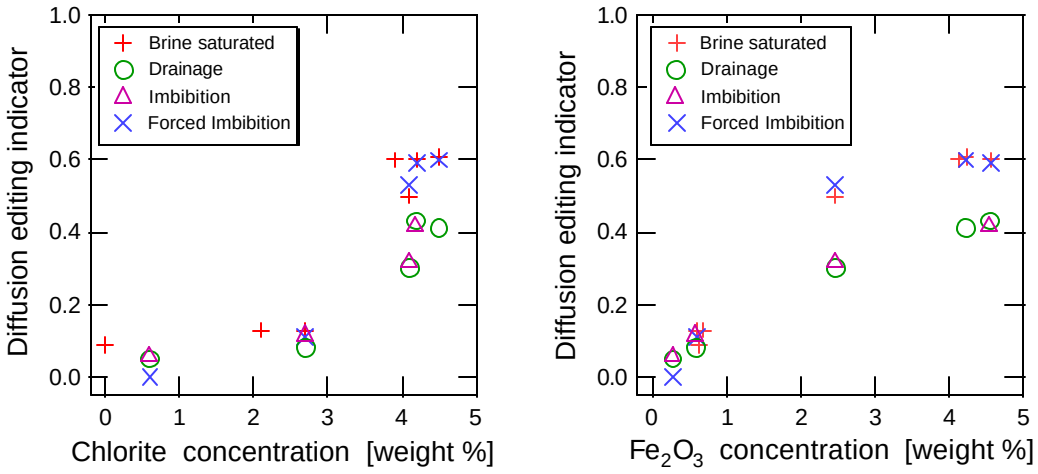

Figure 7. Chlorite indicator from diffusion editing versus chlorite concentration from FTIR (left) and iron concentration from chemical analysis (right).

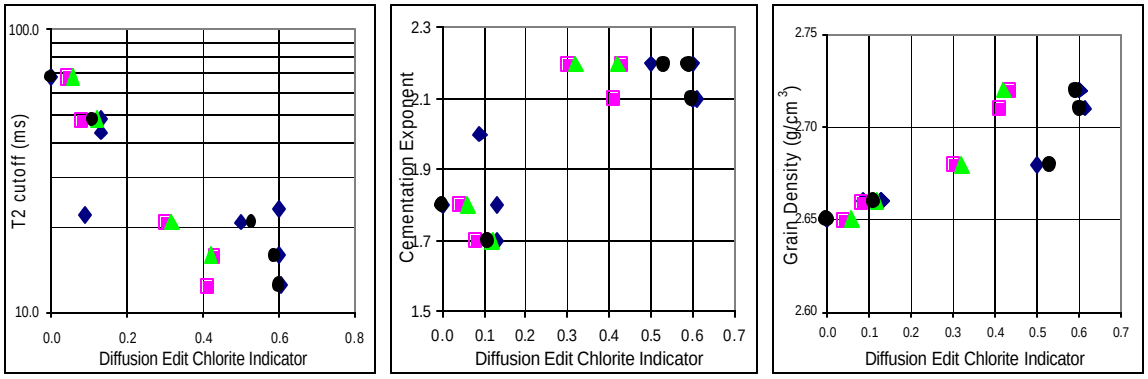

Figure 8. T_2 cutoff (left), cementation exponent (center) and grain density (right) versus chlorite indicator from diffusion editing (brine = diamonds; drainage = squares; spontaneous imbibition = triangles; forced imbibition = circles).